Journal of Pharmacokinetics and Biopharmaceutics, Vol. 16, No. 6, 1988

Competing Pathways in Drug Metabolism. II. An Identical, Anterior Enzymic Distribution for 2- and 5-Sulfoconjugation and a Posterior Localization for 5-Glucuronidation of Gentisamide in the Rat Liver

Marilyn E. Morris,[1,3] Vincent Yuen,[1] and K. Sandy Pang[1,2,4]

Received March 18, 1988—Final July 11, 1988

Gentisamide (2,5-dihydroxybenzamide, GAM), a substrate that forms two monosulfates at the 2 and 5 positions (GAM-2S and GAM-5S) and a monoglucuronide at the 5 position (GAM-5G), was delivered at 8 or 80 μM by normal (N) and retrograde (R) flows to the once-through rat liver preparation. At the lower (8 μM) input concentration, ratios of conjugate formation rate, GAM-5S/GAM-5G and GAM-2S/GAM-5G, were decreased significantly (4.01 ± 1.42 to 2.93 ± 0.99, and 1.13 ± 0.65 to 0.66 ± 0.41, respectively) whereas a small but significant increase in the steady-state extraction ratio, E (0.89 ± 0.029 to 0.94 ± 0.016), was observed upon changing the flow direction from N to R. At the higher input GAM concentration (80 μM), conjugate formation rate ratios were relatively constant for GAM-5S/GAM-5G (1.18 ± 0.08 to 1.11 ± 0.12) and GAM-2S/GAM-5G (0.33 ± 0.05 to 0.31 ± 0.05) upon changing flow direction from N to R, despite a slight increase in E from 0.87 ± 0.023 to 0.91 ± 0.016 was observed. These results suggest that the sulfotransferase activities responsible for 2- and 5-sulfoconjugations are identically distributed and localized anterior to 5-glucuronidation activities during a normal flow of substrate into the rat liver (entering the portal vein and exiting the hepatic vein), and that the presence of uneven distribution of conjugation activities is discriminated only at the lower input drug concentration. At high concentration (> K_m for all systems), saturation of all pathways occurs, and other anteriorly/identically distributed competing pathways would fail to perturb downstream intrahepatic drug concentrations and the resultant conjugation rates. The lack of change in

The work was supported by the Medical Research Council of Canada (DG-263 and MA-9104) and a grant from the Canadian Liver Foundation. M. E. Morris was a recipient of a MRC post doctoral fellowship.

[1]Faculty of Pharmacy, University of Toronto, Toronto, Ontario, Canada.
[2]Department of Pharmacology, Faculty of Medicine, University of Toronto, Toronto, Ontario, Canada
[3]Present address: Department of Pharmaceutics, School of Pharmacy, State University of New York at Buffalo, Amherst, New York 14260.
[4]To whom correspondence should be sent at Faculty of Pharmacy, 19 Russell Street, University of Toronto, Toronto, Ontario, Canada M5S 2S2.

0090-466X/88/1200-0633$06.00/0

metabolic profiles renders the condition unsuitable for examination of uneven distribution of enzymes in the liver. These observations were generally predicted by theoretical enzymic models of consistent distribution patterns. Because 2- and 5-sulfation were mediated by systems of similar K_m but different V_{max} values, two possibilities, the same isozyme of sulfotransferase being involved in the formation of two enzyme-substrate complexes to form two distinctly different products or two isozymes of sulfotransferases of identical distribution, were discussed.

KEY WORDS: competing pathways; sulfation and glucuronidation; gentisamide conjugation; K_m and V_{max}; substrate recruitment of hepatocyte activity; input concentration; enzymic distribution patterns; anterior or posterior; isozyme; enzymic distribution models.

INTRODUCTION

The phenomenon of zonal distribution of metabolizing enzymes of drugs and endogenous compounds within the liver is well established. Hepatocytes of acinar zones 1 (periportal) and 3 (perivenous or pericentral), as described by Rappaport (1,2), are heterogeneous with respect to structure, enzyme content, and most likely function (3,4). Hepatocytes of acinar zone 1 are generally involved in gluconeogenesis and bile salt transfer whereas those of zone 3 participate in glycolysis and lipid metabolism (5–8). Hepatocytes from all zones of the liver mediate drug metabolism, albeit to varying extents. In most cases, perivenous hepatocytes are important for Phase I and Phase II (glucuronidation and glutathione conjugation) reactions (9–15). Sulfoconjugation, however, is predominantly located in the periportal liver acinus (15–17). An understanding of enzymic distribution patterns within the liver is important, as it lends insight into sequential metabolism (13,18) as well as the nature and proportions of metabolites formed in competing, parallel pathways (19–23). For the latter case, zonal distribution of metabolizing enzymes can significantly modulate the intrahepatic substrate concentrations and therefore influence the extraction and metabolism of a drug biotransformed by two or more parallel (competing) pathways (22,23).

Gentisamide (2,5-dihydroxybenzamide, GAM) is metabolized to three metabolites, gentisamide-5-glucuronide (GAM-5G), gentisamide-5-sulfate (GAM-5S), and gentisamide-2-sulfate (GAM-2S) in the single-pass perfused rat liver preparation when varying input GAM concentration (0.9 to 450 μM) was delivered at 10 ml/min (20). The extraction ratio of GAM at low input concentrations (C_{In}) is high (generally about 0.9) and remains constant at C_{In} up to about 120 μM. Despite this constant E, nonlinear formation of the metabolites is present: With increasing C_{In}, GAM-5G increases disproportionately and at the expense of GAM-5S and GAM-2S. After fitting the conjugation rates to the Michaelis-Menten equation, with the logarithmic average concentration serving as an estimate of the mean

concentration in liver, the enzymatic parameters for metabolite formation are (K_m values have been corrected for GAM binding):

GAM-2S, $K_m = 22 \pm 14\ \mu M$, $V_{max} = 287 \pm 117$ nmol/min per liver;

GAM-5S, $K_m = 26 \pm 12\ \mu M$, $V_{max} = 978 \pm 306$ nmol/min per liver;

GAM-5G, $K_m = 71 \pm 22\ \mu M$, $V_{max} = 1062 \pm 465$ nmol/min per liver.

Despite the similarities in K_m values for the sulfation pathways and a lack of a demonstrable trend in the ratio of GAM-5S/GAM-2S (mean was 3.56) with concentration, the data would not discern the distribution patterns for the conjugation activities nor whether the same isozyme of sulfotransferase is responsible for 2- and 5-sulfation. Because of the increasing dominance of GAM-5G at the expense of GAM-2S and GAM-5S with increasing GAM concentration, the pattern is consistent with either (i) an even or identical distribution of conjugation enzymes, with a higher K_m for glucuronidation, or (ii) uneven distribution of enzymatic activities, that is, an anterior sulfation and a posterior glucuronidation system (20,23).

GAM metabolism in the single-pass perfused rat liver is presently employed to exemplify the importance of both enzymatic parameters and enzymic distributions for conjugate formation. In this investigation, we employed the technique of retrograde rat liver perfusion (substrate entry into the hepatic vein and exit by the portal vein) to probe the relative enzymic distribution patterns of conjugation activities for GAM, a compound metabolized by three parallel pathways. With retrograde (R) delivery of substrate, the localization of enzymic activities along the flow path is reversed relative to normal (N) perfusion (entry into the portal vein and exit by way of hepatic vein) in influencing metabolite formation. If enzymic distributions are evenly distributed within the liver acinus, no change is expected in the ratio of conjugates formed for N and R. However, a decrease in the ratio of metabolite formation (conjugate I/conjugate II) during R in comparison to N suggests a posterior distribution of activities for conjugate II formation (24,25).

The manner in which a high-affinity anterior pathway (I) and a low-affinity posterior system (II) affects metabolite formations with N vs. R flows has been explored by computer simulations (22,23). With R, the following should be observed: At low C_{In} ($<$ all apparent K_m values where $K_{m,app}$ is the true K_m/unbound fraction in blood), the greatest decrease in metabolite formation (I/II) occurs without a significant change in drug extraction ratio, E; at intermediate C_{In} ($> K_{m,app}$ for the anterior pathways and $< K_{m,app}$ for the posterior pathway), a decrease in metabolite ratio (I/II) but an increase in E results: at high C_{In} ($>$ all $K_{m,app}$'s), metabolite ratio and E remain unchanged. The expectations are due to the varying extents of modulation of intrahepatic substrate concentration at any point

x in liver by events at or preceding x when the input substrate concentration is varied. The intrahepatic substrate concentration varies as a result of drug processing by enzymatic pathways, with the enzymatic constants, input substrate concentration, as well as enzyme localizations as major determinants. The varying effects of low vs. high C_{In} on metabolite formation and E during both N and R are due to whether a large intrahepatic gradient of substrate concentration exists in the liver. If such a gradient exists, the modulating effects of competing, anterior pathways is great, as substrate is efficiently removed to prevent substrate recruitment of downstream hepatocyte activity. In an absence of such a gradient, a high intrahepatic substrate concentration exists at all points in the liver to allow for recruitment of all hepatocyte activity, and hence, the modulating effects from competing pathways arising from differences in enzymic distributions and K_m values become unimportant.

Therefore, we chose to examine two different input concentrations in our experiments to contrast the influence of enzymic distributions and K_m values for competitive pathways under low and high input substrate concentrations: a low C_{In} (8 μM) where $C_{In} < K_{m,app}$'s of all pathways, and a high C_{In} (80 μM) where the $C_{In} > K_{m,app}$'s for the formation of GAM-5S and GAM-2S but $< K_{m,app}$ for the formation of GAM-5G. Computer modeling, based on the K_m and V_{max} values estimated from our liver perfusion studies (20), was used to simulate data (E and metabolite ratios) with different enzymic distribution patterns. These simulations do not assume the same isozyme of sulfotransferse mediating both 2- and 5-sulfoconjugations.

MATERIALS AND METHODS

Chemicals

GAM was synthesized according to Morris and Levy (26) by the method of Faust *et al.* (27). ^{3}H-GAM (specific activity, 39 mCi/mmol) was a product obtained by catalytic exchange with tritiated water from New England Nuclear, Boston, MA. Aliquots of ^{3}H-GAM were further purified by thin-layer chromatography before use (20), and the radiochemical purity of ^{3}H-GAM was greater than 95%. All other reagents and solvents (Burdick and Jackson, Muskegon, MI) were of HPLC grade.

Perfused Liver Studies

The single-pass *in situ* perfused rat liver preparation was used, as previously described (20). Male Sprague-Dawley rats, weighing 312–379 g (Charles River, St. Constant, Quebec) served as liver donors. Blood perfusate consisted of 20% washed human red blood cells, 1% albumin, and

300 mg% glucose in Krebs-Henseleit bicarbonate (KHB) buffer. The perfusate was delivered at a constant flow rate of 10 ml/min per liver in normal perfusion (via the portal vein) or in a retrograde direction (via the inferior vena cava into the hepatic vein). Each rat liver was studied for three experimental periods each of 45-min duration, with identical first and last periods (either both normal or retrograde perfusion). Preliminary studies established that steady state was achieved within 20 min. Four output (hepatic venous) blood samples (C_{Out}) were collected at 3-min intervals under steady-state conditions, beginning at 33 min, and two input (C_{In}) blood samples were collected during this interval. Bile samples were collected between 25–30, 30–35, 35–40, and 40–45 min.

Viability of the liver preparation was assessed in some experiments by examining glutamic oxaloacetic transaminase (SGOT) and glutamic pyruvic transaminase (SGPT) and K^+ and glucose among inflow and outflow perfusate samples. No significant changes in these parameters were found in these studies. Metabolic activity, estimated by the steady-state hepatic drug extraction ratio, E, during the first and last identical experimental periods was also compared to ensure that hepatic function had not altered during the time course of each liver perfusion.

Two sets of experiments were conducted to examine the effects of input concentration and flow direction on the extraction ratio and metabolism of GAM. The first series of six experiments examined metabolism at an input concentration (C_{In}) of approximately 8 μM (6.5–12.7 μM) while the second series of four experiments utilized a 10-fold higher C_{In} (68.9–97.1 μM). The two concentrations furnished varying input substrate concentrations compared to the $K_{m,app}$'s of the systems ($<K_{m,app}$'s of all pathways and $>K_{m,app}$ for sulfation and $<K_{m,app}$ for glucuronidation; (the apparent K_m is the true K_m/f_B, where f_B is the unbound fraction in blood). Steady-state metabolite formation rates were obtained by summing the biliary excretion rate and the rate of appearance of metabolite in the perfusate (product of the output concentration and blood flow). The rate of metabolite formation was expressed as a percentage of the rate of input of drug, determined at steady state. The extraction ratio of GAM was determined in blood samples as described in Eq. (6).

Statistical analysis of extraction ratios and metabolite ratios was performed by paired t tests. The results of the first and last experimental periods, which represented identical experimental conditions, were averaged for the statistical analyses. A p value of <0.05 was taken as significant.

Analytical Procedures

GAM and its metabolites in plasma and bile were separated by HPLC, and the radioactivities present in the collected eluant fractions were determined by liquid scintillation counting, as previously reported (20). Briefly,

separation of GAM and its metabolites was achieved using a mobile phase consisting of 1% acetic acid and 8% methanol in 0.1 M KH_2PO_4 at a flow rate of 1.0 ml/min on a μBondapak C_{18} column (Waters Associates, Mississauga, Ont.). Perfusate plasma samples were analyzed following protein precipitation with 1 M perchloric acid. Bile samples were analyzed following the addition of 40 μl of 20% methanol in water solution to 20 μl of bile. HPLC fractions corresponding to the metabolites and GAM were collected, added to scintillation fluor and counted. Labeled and unlabeled GAM from afferent and efferent blood samples were quantitated by scintillation counting and HPLC, respectively, following extraction with ethyl acetate.

Simulations

Simulations for single-pass liver perfusion, based on numerical approximations as previously described (22,23), were performed to examine the effects of enzyme distribution patterns, direction of flow, and the input substrate concentration on the extraction ratio and metabolism of GAM in the liver perfusion system. The liver is assumed to comprise sinusoids of similar lengths and capillary transit times (28) such that each sinusoid receives an equal fraction of the total liver blood flow. The K_m for each metabolite is assumed to be constant among hepatocytes lining the sinusoids, but the amount of enzyme, or $V_{max,x}$, at any point x can vary from one hepatocyte to the next depending on the enzyme distribution pattern. In these simulations, total liver blood flow may be viewed as bulk flow through an effective single sinusoid with a distribution of $V_{max,x}$ along L, the length of the sinusoid. The length-averaged V_{max} is given by

$$V_{max} = \int_0^L V_{max,x}\, dx/L \tag{1}$$

where $V_{max,x}$ represents the amount of enzyme within a cell at any point, x, and dx is a small increment in distance along L.

A condition similar to the single-pass liver perfusion system, with a constant input concentration of drug (C_{In}) delivered at a constant blood flow rate, Q (10 ml/min per liver), was examined under steady-state conditions using mass balance relationships. Additional assumptions in the simulations included: (i) Diffusional transport and cofactor(s) are not rate-limiting. (ii) Binding of drug in blood at varying drug concentrations is constant. This is true for GAM, and the unbound fraction in blood, f_B, is 0.516 (20). The rate of drug disappearance at steady state at any point, x, v_x, is represented by the combined rates of sulfation (v_x^{2S}, v_x^{5S}) and glucuroni-

dation (v_x^{5G}) at point x.

$$\frac{Q\,dC_x}{dx} = v_x = v_x^{2S} + v_x^{5S} + v_x^{5G}$$

$$= -\frac{1}{L}\left\{\frac{V_{max,x}^{2S}\,C_x}{K_m^{2S}/f_B + C_x} + \frac{V_{max,x}^{5S}\,C_x}{K_m^{5S}/f_B + C_x} + \frac{V_{max,x}^{5G}\,C_x}{K_m^{5G}/f_B + C_x}\right\} \tag{2}$$

where superscripts 2S, 5S, and 5G represent GAM-2S, GAM-5S, and GAM-5G, respectively, and C_x is the drug concentration at point x. The output drug concentration was given by C_x at $x = L$.

The length-averaged metabolite formation rates are given by the following equations:

$$\bar{v}^{2S} = \int_0^L \frac{V_{max,x}^{2S} C_x}{(K_m^{2S}/f_B + C_x)} \frac{dx}{L} \tag{3}$$

$$\bar{v}^{5S} = \int_0^L \frac{V_{max,x}^{5S} C_x}{(K_m^{5S}/f_B + C_x)} \frac{dx}{L} \tag{4}$$

$$\bar{v}^{5G} = \int_0^L \frac{V_{max,x}^{5G} C_x}{(K_m^{5G}/f_B + C_x)} \frac{dx}{L} \tag{5}$$

The steady-state extraction ratio of GAM, E, is calculated by

$$E = \frac{C_{In} - C_{Out}}{C_{In}} \tag{6}$$

Five enzyme distribution patterns, from the input to output of the liver for each of the pathways are described (Fig. 1): (A) is an evenly distributed system : (B), the activity decreases linearly from input to output, dwindling to zero activity at the output; (C), the activity decreases linearly, with activity at input being three times that for output; (D), the activity increases linearly from zero at input; (E), the activity increases linearly, with activity at input being one-third that at the output. Possible combinations of these five distribution patterns (A to E, Fig. 1) were used to describe the patterns of enzymic distribution patterns, and the model was named with the first, second, and third letters for the model denoting the distribution patterns for GAM-2S, GAM-5S, and GAM-5G formation, respectively. For example, model ABC represents an evenly distributed system for GAM-2S formation, a linearly decreasing (to zero) gradient of GAM-5S activity, and a linearly decreasing gradient for GAM-5G from input to output (one-third of original input value). In these simulations, 500 steps were used in the numerical approximation.

Two sets of simulations were performed: Set I contained models with identical distributions of sulfation activities that are anterior to glucuronidation activities and Set II described models without these constraints. The

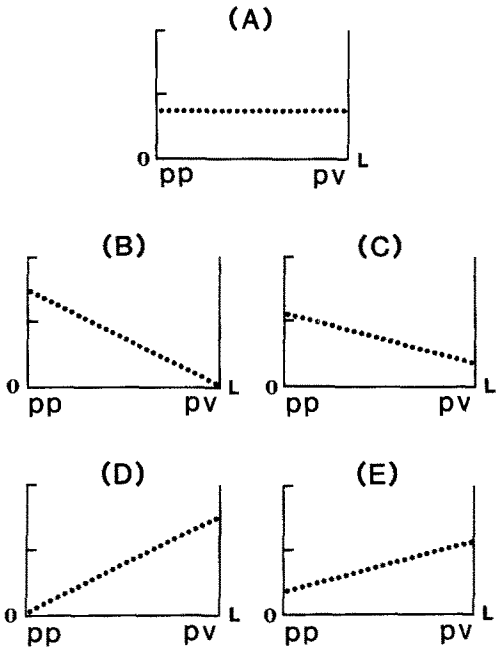

Fig. 1. Schematic illustration (to scale) for the same amount of enzyme, distributed in five possible patterns, (A) to (E). The y axis is the amount of enzyme (or $V_{max,x}$) and the dotted lines denote the distribution pattern along the sinusoidal flow path from the input (0) to output (L) of the liver (x axis); pp and pv represent the periportal and perivenous regions, respectively.

enzymatic parameters (apparent V_{max} and K_m values) derived for the three metabolic pathways (20) were used to simulate E and the ratios of metabolites (GAM-5S/GAM-5G, GAM-5S/GAM-2S, and GAM-2S/GAM-5G) formed at steady state with N and R for C_{In}'s at 8 and 80 μM for these models. The least sum of squares of weighted residuals between predictions and observations for these parameters was used to define the best model of enzymic distribution.

Some of the models were further tested for consistency with data published previously when stepwise changes in C_{In} were made to the single-pass rat liver preparations at constant flow (20). The K_m and V_{max} values for GAM conjugations were again utilized with the enzymic distribution patterns to predict conjugation rates upon varying C_{In} from 0.1 to 500 μM for comparison with observations.

RESULTS

Viability

When GAM was perfused in normal and retrograde directions at input concentrations of approximately 8 and 80 μM, the first and last experimental periods were identical for all liver preparations, evidenced by the constancy in E of GAM (Tables I and II), suggesting little change in liver viability over the time of the experiment. Liver viability, as assessed by other measures (appearance; enzyme, K^+, and glucose in inflow and outflow perfusate concentrations; microscopy), confirmed these findings.

Table I. Effect of Direction of Flow on the Steady-State Extraction Ratio and the Ratios of Metabolites When a Low Gentisamide Input Concentration (6.5–12.7 μM) Was Delivered to the Once-Through Perfused Rat Liver (10 ml/min)

Expt. no.	Direction of flow[a]	Steady-state extraction ratio of GAM[b] E	Ratio of rates of metabolite formation at steady state		
			GAM-5S / GAM-5G	GAM-5S / GAM-2S	GAM-2S / GAM-5G
5	N	0.878 ± 0.004	5.05 ± 0.21	2.82 ± 0.26	1.95 ± 0.52
	R	0.913 ± 0.007	3.99 ± 0.21	3.06 ± 0.12	1.31 ± 0.11
	N	0.791 ± 0.019	5.11 ± 0.55	2.91 ± 0.15	1.76 ± 0.23
6	N	0.870 ± 0.011	6.00 ± 0.13	3.48 ± 0.17	1.73 ± 0.07
	R	0.957 ± 0.002	4.81 ± 0.32	3.56 ± 0.08	1.35 ± 0.11
	N	0.935 ± 0.003	5.60 ± 0.13	3.17 ± 0.13	1.77 ± 0.05
8	R	0.937 ± 0.005	2.44 ± 0.19	5.21 ± 0.12	0.47 ± 0.05
	N	0.914 ± 0.001	3.44 ± 0.25	4.99 ± 0.22	0.69 ± 0.07
	R	0.930 ± 0.001	2.65 ± 0.10	4.87 ± 0.07	0.54 ± 0.03
9	R	0.914 ± 0.002	2.56 ± 0.06	5.97 ± 0.33	0.43 ± 0.03
	N	0.906 ± 0.002	3.61 ± 1.14	5.45 ± 0.24	0.57 ± 0.05
	R	0.942 ± 0.004	3.59 ± 0.21	4.87 ± 0.44	0.74 ± 0.10
14	N	0.841 ± 0.004	2.42 ± 0.66	3.72 ± 0.20	0.66 ± 0.21
	R	0.949 ± 0.001	1.90 ± 0.06	3.59 ± 0.09	0.53 ± 0.01
	N	0.893 ± 0.003	2.32 ± 0.35	3.41 ± 0.55	0.71 ± 0.23
24	R	0.946 ± 0.001	2.46 ± 0.36	7.61 ± 1.40	0.34 ± 0.10
	N	0.882 ± 0.003	2.66 ± 0.44	7.04 ± 0.91	0.35 ± 0.14
	R	0.921 ± 0.003	1.93 ± 0.30	8.88 ± 1.49	0.23 ± 0.08
	N *vs.* R	$p < 0.005$	$p < 0.002$	ns	$p = 0.05$

[a] N and R, respectively, denote normograde and retrograde perfusions.

[b] Mean ± *SD* of 4 determinations. For all studies, mean E, and formation rates of GAM-2S, GAM-5S, and GAM-5G during N were 0.886 ± 0.029, and 13.8 ± 4.7, 58.4 ± 5.5, and 17.1 ± 5.5 nmol/min, respectively; the corresponding values during R were 0.936 ± 0.016 and 14.2 ± 4.4, 58.6 ± 4.1, and 21.0 ± 6.0 nmol/min, respectively.

Table II. Effect of Direction of Flow on the Steady-State Extraction Ratio and the Ratios of Metabolites When a High Gentisamide Input Concentration (68.9-97.1 μM) Was Delivered to the Once-Through Perfused Rat Liver (10 ml/min)

Expt. no.	Direction of flow[a]	Steady-state extraction ratio of GAM[b] E	Ratio of rates of metabolite formation at steady-state		
			GAM-5S / GAM-5G	GAM-5S / GAM-2S	GAM-2S / GAM-5G
19	N	0.867 ± 0.002	1.10 ± 0.08	3.87 ± 0.22	0.28 ± 0.01
	R	0.914 ± 0.001	1.00 ± 0.07	2.92 ± 0.26	0.35 ± 0.03
	N	0.868 ± 0.003	1.06 ± 0.12	2.95 ± 0.26	0.36 ± 0.06
20	N	0.838 ± 0.007	1.17 ± 0.05	3.85 ± 0.12	0.31 ± 0.02
	R	0.895 ± 0.004	1.04 ± 0.04	4.02 ± 0.29	0.26 ± 0.02
	N	0.853 ± 0.004	1.21 ± 0.08	4.26 ± 0.48	0.29 ± 0.04
21	R	0.911 ± 0.003	1.14 ± 0.07	4.21 ± 0.28	0.27 ± 0.01
	N	0.853 ± 0.004	1.27 ± 0.03	4.06 ± 0.29	0.32 ± 0.02
	R	0.902 ± 0.001	0.98 ± 0.11	3.86 ± 0.42	0.26 ± 0.03
22	R	0.938 ± 0.001	1.20 ± 0.06	3.14 ± 0.32	0.38 ± 0.04
	N	0.897 ± 0.002	1.24 ± 0.08	2.86 ± 0.33	0.42 ± 0.02
	R	0.928 ± 0.002	1.27 ± 0.03	3.62 ± 0.28	0.35 ± 0.03
	N *vs.* R	$p < 0.002$	ns	ns	ns

[a] N and R, respectively, denote normograde and retrograde perfusions.
[b] Mean ± SD of 4 determinations. For all studies, mean E, and formation rates of GAM-2S, GAM-5S, and GAM-5G during N were 0.866 ± 0.023, and 11.5 ± 1.2, 40.4 ± 2.9, and 34.2 ± 4.0 nmol/min, respectively; the corresponding values during R were 0.912 ± 0.016 and 11.1 ± 1.6, 39.6 ± 0.9, and 36.6 ± 2.8 nmol/min, respectively.

Low C_{In}

At a C_{In} of 8 μM, the extraction ratio for GAM increased from 0.886 ± 0.029 to 0.936 ± 0.016 (mean ± SD, $p < 0.005$) from N to R. During N, GAM-5S was the major metabolite, and accounted for 58.4 ± 5.5% (mean ± SD) of total output at steady state; the proportions of GAM-5G and GAM-2S were 17.1 ± 5.5% and 13.8 ± 4.7% of total output rate, respectively (sum of metabolite formation rates and the efflux rates of unconjugated GAM into bile and perfusate). During R, the proportion of GAM-5G increased (21.06 ± 6.0% of total output rate $p < 0.005$), whereas those for GAM-5S and GAM-2S were similar (58.6 ± 4.1% and 14.2 ± 4.4% of total output rate, respectively) relative to those for N. The ratios of the steady-state formation rates of sulfate/glucuronide, GAM-5S/GAM-5G and GAM-2S/GAM-5G, decreased significantly upon changing from N to R. But the ratio of formation rates of the sulfates, GAM-5S/GAM-2S, remained unaltered for both flow directions for each liver preparation, despite the variability observed among different preparations (Table I, Fig. 2).

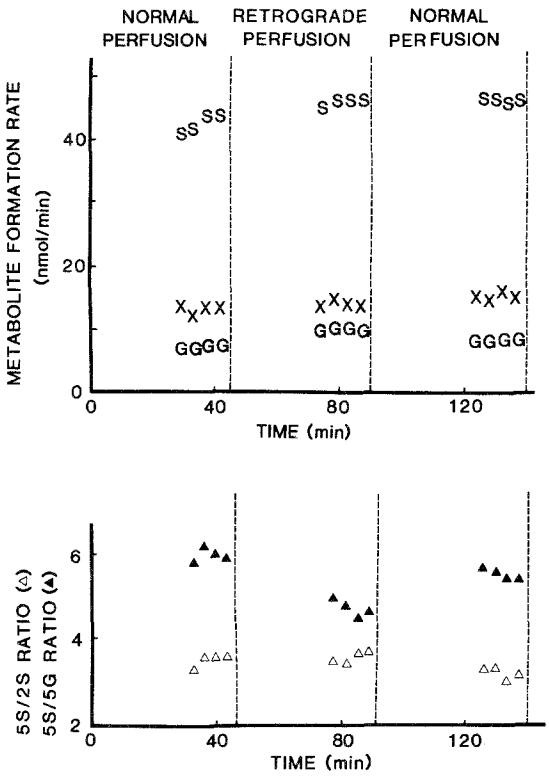

Fig. 2. The rates of formation of gentisamide conjugates with normal (normal) and retrograde perfusions during three steady-state periods (45 min) of normal, retrograde, and normal perfusions to a representative perfused rat liver preparation (flow rate = 10 ml/min; $C_{In} \cong 8\ \mu M$). S, X, and G represent GAM-5S, GAM-2S, and GAM-5G, respectively.

High C_{In}

At a C_{In} of 80 μM, the extraction ratios increased upon changing from N to R (0.866 ± 0.023 and 0.912 ± 0.016, respectively, $p < 0.002$). Although these E's at 80 μM were similar to that observed for both N and R at 8 μM, the proportions of metabolites differed. At this higher C_{In} of GAM, the proportions of GAM-5S, GAM-5G, and GAM-2S now accounted for 40.4 ± 2.9, 34.2 ± 4.0, and $11.5 \pm 1.2\%$, respectively, of total output rate during normal perfusion. No significant change in the metabolic profile, and hence the ratio of metabolites, was seen after retrograde perfusion (Table II).

When data at input concentrations of 8 vs. 80 μM for each directional flow were compared, E was unchanged for normal flow, whereas a small

but significant decrease was observed for retrograde perfusion (cf. Tables I and II). Significant changes in metabolite profile were noted at these two input concentrations: Formation rate of GAM-5S was significantly decreased and that of GAM-5G was significantly increased when C_{In} was increased from 8 to 80 μM for both normal and retrograde perfusions. The proportion of GAM-5S was significantly decreased and that of GAM-5G, increased after increasing C_{In} from 8 to 80 μM, following either normal and retrograde perfusions, whereas the proportions of GAM-2S was unchanged. These results are also consistent with a changing metabolic pattern for GAM previously seen with increasing C_{In} with normal flow (20). A striking observation was that the ratio of GAM-5S/GAM-2S had remained relatively constant at 8 and 80 μM and for each flow direction.

Interpretation of Kinetic Data

The constancy in GAM-5S/GAM-2S during both normal and retrograde flows (Tables I and II) and previous data on GAM metabolism with increasing GAM concentrations with normal perfusion (20) suggest an identical distribution of GAM sulfation activities. The combined data also revealed these activities as distributed anterior to glucuronation activities, and that these sulfation activities are of similar K_m but different V_{max} values. These properties raise the question whether the same isozyme of sulfotransferase is responsible in mediating the regio-sulfoconjugation (2 and 5 positions) of GAM. The behavior of this kinetic system ((Fig. 3), involving one enzyme but two enzyme substrate complexes (ES_1 and ES_2) for formation of two distinct products (P_1 and P_2), is described in the Appendix. The analysis (Appendix) suggests that if the same isozyme of rat liver sulfortansferase is responsible for GAM 2- and 5-sulfoconjugations, the (apparent) K_m values and distribution patterns of sulfation activities should be identical. Moreover, the ratio, GAM-5S/GAM-2S, should stay relatively constant with C_{In} and direction of flow, and remains similar from preparation to preparation, that is, even when individual activity for GAM-5S and GAM-2S formation varies, the ratio remains the same constant (29,30). Most of these criteria are met by data obtained from this and previous studies within the same rat liver preparation, but variations among preparations were observed (20). Variability in the assay procedure existed for GAM-2S, which was present at low quantities, potentially affecting the estimate of GAM-5S/GAM-2S. The present data are also consistent with two distinct isozymes of similar K_m values and localizations in liver in mediating sulfoconjugation. Whether one single isozyme or two isozymes of sulfotransferases of similar K_m are involved in the sulfoconjugation of GAM is unresolved.

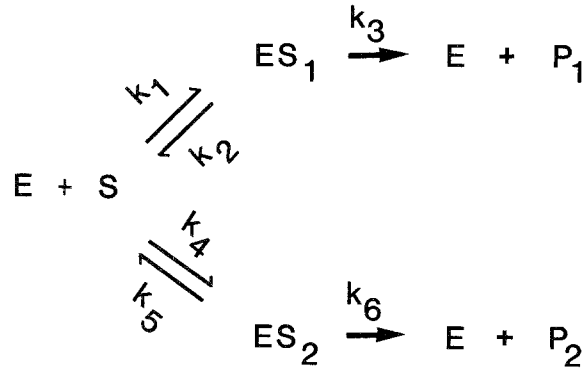

Fig. 3. Formation of multiple metabolites from one isoenzyme, E, and its substrate, S. Two enzyme substrate complexes, ES_1 and ES_2, are in equilibria with free E and S, with forward and backward rate constants, k_1 and k_2 and k_4 and k_5, respectively. These enzyme substrate complexes give rise to products, P_1 and P_2, respectively, with corresponding rate constants, k_3 and k_6.

Simulations

Nine models (AAD, AAE, BBA, BBD, BBE, BBC, CCA, CCD, and CCE), with the constraints of identical distributions of sulfation activities that are anterior to glucuronidation activities (Set I), were examined. These models do not stipulate the same isozyme of arylsufotransferase is responsible for 2- and 5-sulfonconjugation of GAM, but are consistent with data observed from our present experimental studies (Tables I and II). The simulated data (Table III) revealed the following changes upon varying flow from normal to retrograde: at C_{In} of 8 μM, E (>0.96) was nominally increased, GAM-5S/GAM-5G and GAM-2S/GAM-5G were increased but GAM-5S/GAM-2S was the same; at C_{In} of 80 μM, E (>0.88) was slightly increased while small decreases in GAM-5S/GAM-5G and GAM-2S/GAM-5G occurred; but again GAM-5S/GAM-2S remained unchanged. Upon a change in flow direction from N to R, the relative changes in E at 80 μM were greater than the nominal change of E at 8 μM; however, larger changes in the ratios for metabolite formation occurred at 8 μM. A notable observation was the ratio, GAM-5S/GAM-2S, again remained relatively constant at both 8 and 80 μM, as observed for both N and R flows. A ranking of the weighted sum of squares of residuals between the predicted (simulated) and observed E and metabolite ratios (GAM-5S/GAM-5G, GAM-5S/GAM-2S, and GAM-2S/GAM-5G) for all models at 8 and 80 μM revealed that AAE < CCA < BBC < AAD < CCE (Table III).

Other distribution patterns, which describe glucuronidation activities anterior to the sulfation activities, were also employed in the simulations.

Table III. A Comparison of Observed Versus Simulated Data from Models in Set I

	Normal perfusion, 8 μM				Retrograde perfusion, 8 μM			
	E	GAM-5S / GAM-5G	GAM-5S / GAM-2S	GAM-2S / GAM-5G	E	GAM-5S / GAM-5G	GAM-5S / GAM-2S	GAM-2S / GAM-5G
Observations								
Mean	0.886	4.01	4.11	1.13	0.936	2.93	5.29	0.66
±SD	0.029	1.42	1.42	0.65	0.016	0.99	1.93	0.41
Simulations								
Models								
AAD	0.961	4.246	2.899	1.465	0.962	1.623	2.894	0.561
AAE	0.962	3.078	2.898	1.062	0.962	1.941	2.895	0.670
BBA	0.961	3.630	2.897	1.253	0.962	1.448	2.891	0.501
BBC	0.962	2.890	2.897	0.998	0.962	1.820	2.894	0.629
BBD	0.961	7.159	2.898	2.470	0.962	0.995	2.887	0.345
BBE	0.961	4.838	2.898	1.669	0.962	1.187	2.889	0.411
CCA	0.962	2.973	2.897	1.026	0.962	1.884	2.895	0.651
CCD	0.961	5.545	2.899	1.913	0.962	1.291	2.892	0.446
CCE	0.961	3.890	2.898	1.342	0.962	1.540	2.893	0.532

[a] $\frac{1}{\text{predicted}^2}$ was used for weighting.

Table IV. A Comparison of Observed Versus Simulated Data for Models in Set II

	Normal perfusion, 8 μM				Retrograde perfusion, 8 μM			
	E	GAM-5S / GAM-5G	GAM-5S / GAM-2S	GAM-2S / GAM-5G	E	GAM-5S / GAM-5G	GAM-5S / GAM-2S	GAM-2S / GAM-5G
Observations								
Mean	0.886	4.01	4.11	1.13	0.936	2.93	5.29	0.66
±SD	0.029	1.42	1.42	0.65	0.016	0.99	1.93	0.41
Simulations								
Models								
ABC	0.962	2.875	4.346	0.662	0.962	1.801	1.764	1.021
ABD	0.961	6.854	4.263	1.608	0.962	0.963	1.678	0.574
ABE	0.961	4.730	4.291	1.102	0.962	1.155	1.707	0.677
BAC	0.962	1.932	1.970	0.981	0.962	3.040	4.987	0.610
BAD	0.961	4.378	2.012	2.176	0.962	1.637	5.242	0.312
BAE	0.961	3.116	1.998	1.560	0.962	1.949	5.154	0.378
BCD	0.961	5.652	2.440	2.317	0.962	1.302	3.962	0.329
BCE	0.961	3.927	2.432	1.614	0.962	1.550	3.923	0.395
CAD	0.961	4.311	2.383	1.809	0.962	1.630	3.749	0.435
CAE	0.961	3.097	2.373	1.305	0.962	1.945	3.726	0.552
CBA	0.962	3.609	3.476	1.038	0.962	1.433	2.186	0.656
CBD	0.961	7.004	3.459	2.025	0.962	0.979	2.140	0.457
CBE	0.961	4.784	3.467	1.380	0.962	1.171	2.163	0.541
CDE	0.962	1.791	1.453	1.232	0.962	2.868	5.733	0.500
AAA	0.962	2.392	2.896	0.826	0.962	2.392	2.896	0.826
BBB	0.962	2.391	2.896	0.826	0.962	2.392	2.896	0.826
CCC	0.962	2.392	2.896	0.826	0.962	2.392	2.896	0.826
DDD	0.962	2.392	2.896	0.826	0.962	2.391	2.896	0.826
EEE	0.962	2.392	2.896	0.826	0.962	2.392	2.896	0.826

[a] $\frac{1}{\text{predicted}^2}$ was used for weighting.

Normal perfusion, 80 μM				Retrograde perfusion, 80 μM				Weighted sum of squares of residuals
E	GAM-5S / GAM-5G	GAM-5S / GAM-2S	GAM-2S / GAM-5G	E	GAM-5S / GAM-5G	GAM-5S / GAM-2S	GAM-2S / GAM-5G	
0.866	1.18	3.64	0.33	0.912	1.11	3.63	0.31	
0.023	0.80	0.59	0.05	0.016	0.12	0.51	0.05	
0.885	2.343	3.108	0.754	0.894	1.417	3.083	0.460	2.379
0.887	2.041	3.101	0.658	0.892	1.589	3.089	0.514	1.959
0.885	2.315	3.105	0.746	0.894	1.407	3.080	0.457	2.895
0.887	2.027	3.100	0.654	0.892	1.585	3.087	0.513	2.139
0.880	3.138	3.115	1.007	0.899	1.124	3.064	0.367	6.907
0.882	2.675	3.110	0.860	0.897	1.255	3.072	0.409	4.356
0.887	2.035	3.101	0.656	0.892	1.586	3.088	0.514	2.040
0.882	2.703	3.112	0.869	0.896	1.261	3.075	0.410	3.793
0.885	2.332	3.106	0.751	0.894	1.411	3.081	0.458	2.537

Normal perfusion, 80 μM				Retrograde perfusion, 80 μM				Weighted sum of squares of residuals
E	GAM-5S / GAM-5G	GAM-5S / GAM-2S	GAM-2S / GAM-5G	E	GAM-5S / GAM-5G	GAM-5S / GAM-2S	GAM-2S / GAM-5G	
0.866	1.18	3.64	0.33	0.913	1.11	3.63	0.31	
0.023	0.80	0.59	0.05	0.016	0.12	0.51	0.05	
0.889	2.007	3.824	0.525	0.890	1.596	2.557	0.624	6.012
0.882	3.051	3.756	0.812	0.897	1.119	2.469	0.453	10.148
0.884	2.620	3.777	0.694	0.895	1.254	2.499	0.502	7.744
0.890	1.597	2.541	0.629	0.889	2.012	3.805	0.529	3.236
0.883	2.392	2.611	0.916	0.896	1.414	3.900	0.363	4.095
0.885	2.071	2.588	0.800	0.894	1.580	3.866	0.409	2.940
0.881	2.737	2.851	0.960	0.897	1.261	3.454	0.365	4.381
0.884	2.353	2.837	0.829	0.895	1.409	3.443	0.409	2.736
0.884	2.367	2.842	0.833	0.895	1.416	3.451	0.410	2.555
0.886	2.056	2.826	0.727	0.893	1.585	3.441	0.461	1.882
0.886	2.297	3.423	0.671	0.893	1.409	2.782	0.507	3.957
0.881	3.094	3.411	0.907	0.898	1.122	2.741	0.409	7.712
0.883	2.647	3.416	0.775	0.896	1.255	2.762	0.454	5.350
0.889	1.602	2.343	0.684	0.890	1.996	4.304	0.464	5.978
0.889	1.794	3.095	0.580	0.889	1.794	3.095	0.580	2.277
0.890	1.794	3.095	0.579	0.890	1.794	3.095	0.580	2.277
0.889	1.794	3.095	0.580	0.890	1.794	3.095	0.580	2.277
0.890	1.794	3.095	0.580	0.890	1.794	3.095	0.579	2.777
0.890	1.794	3.095	0.580	0.889	1.794	3.095	0.580	2.777

But the simulated data were inconsistent with the observed trends, and hence the results are not reported. Fifteen other models (ABC, ABD, ABE, BAC, BAD, BAE, BCD, BCE, CCC, CAD, CAE, CBA, CBD, CBE, and CDE), which restrain the distribution of sulfation activities to be anterior to glucuronidation activities without constraining identical distributions of sulfation activities, and five models (AAA, BBB, CCC, DDD, and EEE), which show identical conjugation activities, served as counter-examples (Set II, Table IV). The evenly distributed system (AAA) and other models of identical enzymic distributions (BBB, CCC, DDD, and EEE) all showed the same simulated data: E and the metabolite ratios remained unchanged upon a change in direction of flow. Among the 15 unevenly distributed models, some predicted a decrease in E or an increase of GAM-5S/GAM-5G, GAM-5S/GAM-2S, or GAM-2S/GAM-5G with, upon altering flow from normal to retrograde direction, results that are inconsistent with our present observations. Only the models with both anterior, identical distributions for the sulfation system(s) and a posterior glucuronidation system predicted the general trends of the data (Set I). Among these, models AAE and CCA were superior than other models since the predictions incurred the least sum of squares of residuals.

These two enzymic models (AAE and CCA) were further tested for their predictions on rates of formation of conjugates at increasing C_{In}. The enzymatic parameters (K_m and V_{max} values from ref. 20) were employed to simulate formation rates of the metabolites, GAM-2S, GAM-5S, and GAM-5G at C_{In}'s ranging from 0.1 to 500 μM, and these predictions were then compared to previously observed data in the single-pass perfused liver when C_{In} was varied within this concentration range (20). Simulations from both models yielded comparable trends in metabolite formation rates (Fig. 4). The simulated data were similar to the observations in perfused rat liver, where GAM-5S was the major metabolite at all C_{In}'s and represented 58, 40, 30, and 19% of the rate of presentation of GAM at 0.9, 100, 200, and 400 μM, respectively (10 ml/min) (20). These values were similar to the averaged values of 58, 46.4, 34.5, and 21% obtained in the simulations. The corresponding percentages for GAM-5G observed experimentally were approximately 10, 28, 26, and 13% of the presentation rate of GAM, and were similar to the percentages simulated: 18.3, 24.6, 23.9, and 18.1%. In the perfused rat liver, GAM-2S formation rate accounted for 12 to 27% of GAM input rate at low C_{In} (<18 μM) and 3 to 7% of GAM input rate (400 μM). In the simulations, GAM-2S accounted for 20.3 and 6.3% at GAM input C_{In}'s of 1 and 400 μM, respectively. Upon examination of residual plots for rates of formation of GAM-2S, GAM-5S, and total conjugates (Fig. 5) and the sum of squared residuals (comparable for GAM-2S for both models; Model CCA $<$ Model AAE for GAM-5G; Model

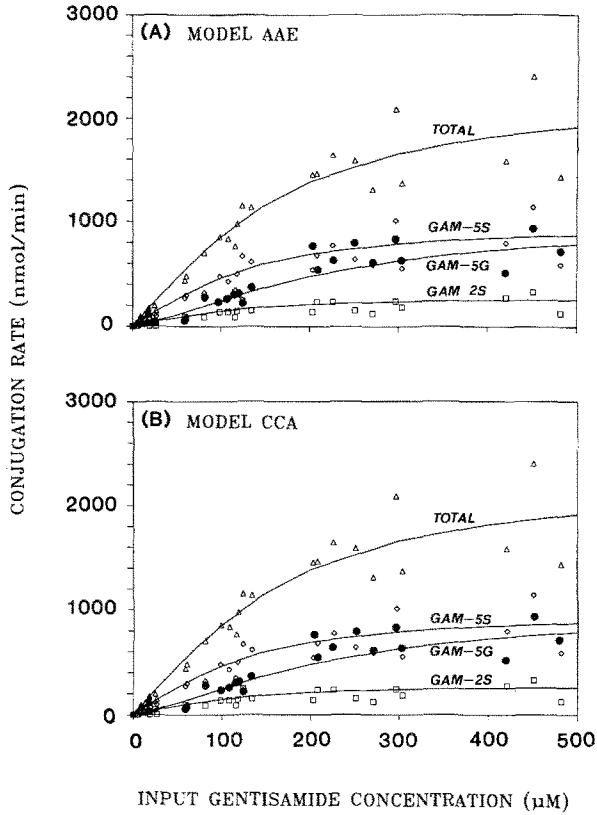

Fig. 4. Predicted and observed formation rates of GAM metabolites. Models AAE (A) and CCA (B), and the enzymatic parameters (GAM-2S, $K_m = 22\ \mu M$, $V_{max} = 287$ nmol/min per liver; GAM-5S, K_m 26 μM, $V_{max} = 978$ nmol/min per liver; GAM-5G, $K_m = 71\ \mu M$, $V_{max} = 1062$ nmol/min per liver) were used to simulate GAM metabolism (solid lines) in the single-pass perfused rat liver, and were compared to observed data (GAM-2S = □; GAM-5S = ◇; GAM-5G = ●; total conjugation rate = △) (observations were taken from ref. 20).

CCA < Model AAE for GAM-5S; Model CCA < Model AAE for total conjugation rate), Model CCA was found to be the better model.

DISCUSSION

In this investigation we have used the technique of normal and retrograde perfusion to examine the enzyme distribution patterns of conjugation activities of GAM, a compound metabolized by three parallel (competing)

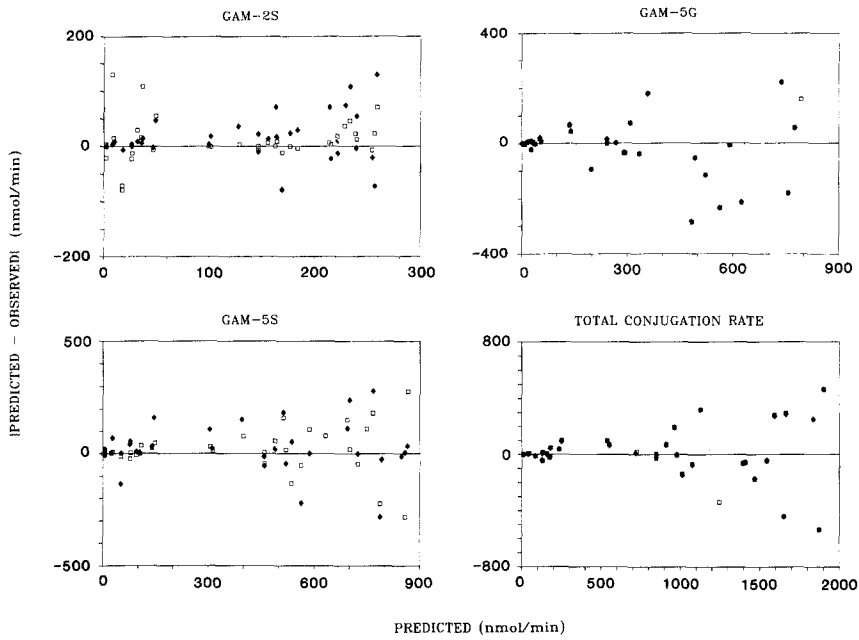

Fig. 5. Residual plots of data for steady-state formation rates of GAM-2S, GAM-5S, GAM-5G, and total conjugation rate of gentisamide upon varying input GAM concentrations to the single-pass rat liver (data taken from Fig. 4). Data for Models AAE and CCA were denoted by □ and ◆, respectively. The sum of squared residuals were for GAM-2S, 67370 and 67296 for Models AAE ane CCA, respectively; for GAM-5G, 365496 and 341371 for Models AAE and CCA, respectively; for GAM-5S, 651730 and 412385, respectively; for total conjugation rate, 1219429 and 1167602, respectively [units were $(nmol/min)^2$].

pathways. Retrograde perfusion of the rat liver preparation does not adversely affect liver function (13,31,32). There was no difference found in the intracellular water space (32), oxygen uptake, mean bile flow, average bile acid excretion, urea synthesis, release of lactic dehydrogenase, glucose secretion (31-33), redox ratios (31,33), biliary excretion of dibromosulfophthalein, DBSP (34), and ethanol (32) and acetaminophen metabolism (13) between N and R. Although retrograde perfusion causes a greater degree of vascular distension in livers perfused either with oxygenated Ringer's solution or blood perfusion medium (31, 32), hepatic ultrastructure was mostly preserved (31,32). By reversing the direction of perfusion, one reverses the relationship between the drug concentration gradient and the hepatocytes along the length of sinusoids. With retrograde perfusion, metabolic activity in the acinar zone 3 or perivenous regions would be recruited before that in the periportal regions. This can result in differences in the steady-state drug extraction ratio and formation of metabolites for a drug

metabolized by more than one metabolic pathway when enzymes are heterogeneously distributed. The phenomenon has been observed in the conjugations of harmol (13,25,35), 7-hydroxycoumarin (15,24), salicylamide (21), the removal of bromosulfophthalein (36), biotransformation of lidocaine (37), and the metabolism of endogeneous compounds such as taurocholate (38) and glutamine (39).

Data from the two sets of experiments (8 and 80 μM) with normal and retrograde flows reveal a significant change in sulfate/glucuronide ratios at C_{In} of 8 μM but not 80 μM, and increases in E (cf. Tables I and II). The sensitivity of metabolite ratios at the lower C_{In} to the change in flow direction is due to the substrate concentration being less than the apparent K_m values for all conjugation systems, whereby enzymic distribution and the K_m are more prone to alter the intrahepatic substrate gradient, and hence, metabolite formation (23). At high C_{In} (80 μM), the ability to discern enzymic distribution patterns with N and R becomes impaired when the enzymic systems are becoming more saturated since less of an intrahepatic gradient exists for the substrate. These trends are readily seen with the present data and previous data on varying GAM and from simulations in the present (Tables III and IV) and previous studies (23).

The data that provided discrimination among the distribution patterns for the conjugation systems (C_{In} at 8 μM) were the ratios of formation rates of GAM-5S/GAM-5G and GAM-2S/GAM-5G, which decreased significantly during retrograde flow while that of GAM-5S/GAM-2S was unchanged. If enzymatic systems are evenly distributed, the steady-state drug extraction ratio and the ratios of metabolite formation rates (sulfation/glucuronidation) should not alter upon reversal of flow (models AAA, BBB, CCC, DDD, and EEE, Table IV). The data also did not agree with an anterior distribution of glucuronidation activity (data not shown) nor with sulfation systems of different distribution patterns (Table IV). But the observed data on GAM metabolism agreed with predictions from models with identical (parallel) distributions of sulfation activities with a posteriorly enriched glucuronidation system (models AAE, CCA, BBC, and AAD, Table III). This kind of relative distribution pattern for sulfation and glucuronidation has been described for other phenolic substrates such as harmol (25,35), 7-hydroxycoumarin (24), and salicylamide (21).

The similarity in K_m for GAM-2S and GAM-5S formation and the identical localization pattern for sulfation activities in liver tend to suggest that the sulfoconjugations may be mediated by a single isozyme of the arylsulfotransferases. The observed ratios of rates of sulfoconjugate formation (GAM-5S/GAM-2S) had remained relatively constant for both flow directions within each experiment regardless of whether C_{In} is at 8 or 80 μM, but these had varied among preparations. The same pattern was also found

in our previous studies where C_{In} was varied stepwise in the same single-pass rat liver preparation (20). These intervariations for GAM-5S/GAM-2S seen among preparations suggest either different detection limitations exist for the metabolites GAM-5S and GAM-2S or that sulfation of GAM is mediated by two forms of sulfotransferases of identical distribution patterns. Although GAM-2S was present at low concentrations at increasing C_{In} and the former explanation is plausible, the second explanation should not be ruled out.

Our corroborated experimental and theoretical data, however, reveal unequivocally that sulfation activities are distributed anterior to glucuronidation activities. At least four enzymic distribution patterns (AAE, CCA, BBC, and AAD; Table III) are consistent with the data. Although model AAE bears the least weighted sum of squares of residuals for the present data, model CCA is better for the prediction of gentisamide conjugation rates with changing C_{In} (20) (Fig. 5). Both models are consistent with the metabolic data. In reality, the enzymic distributions of conjugation activities most probably are continuous and curvilinear, with the relative distribution patterns qualitatively similar to, and yet different from, those defined by the models, which describe linear relationships for the convenience of simulation. Since the enzymic distributions are implied rather than present, qualitative differences between predictions and observations are expected, despite that a general trend consistent with data is obtained (Fig. 4).

The method of NR perfusion provides a general sense of the relative distribution patterns. The anteriorly distributed sulfation pathways, of higher affinities, as in GAM metabolism, effectively modifies intrahepatic GAM concentration in reducing recruitment of downstream glucuronidation activities at low input concentrations, as seen in this study and in previous studies (20). The effectiveness of these sulfation pathways posing as competing pathways for glucuronidation is lessened because of their lower/comparable capacities. Since the K_m (threefold the K_m values for sulfation) and V_{max} for glucuronidation are comparable to those for sulfation (fivefold that for GAM-2S and similar to that for GAM-5S formation), rates of glucuronidation would not change dramatically even when the sulfation pathways are becoming saturated (see data from ref. 20 and Fig. 4). Our present study asserts the importance of an understanding of the interplay among enzymic distribution patterns, the enzymatic constants (K_m and V_{max}), and the input substrate concentration in influencing metabolite formation among competing, parallel pathways, exemplified in the metabolism of gentisamide.

APPENDIX

The kinetic equations underlying the properties of the system for one

enzyme, mediating the formation of two products (P_1 and P_2) via two enzyme-substrate complexes (ES_1 and ES_2), is presently explored. The equilibria concentrations may be expressed as follows

$$[ES_1] = \frac{[E][S]}{(k_2 + k_3)/k_1} = \frac{[E][S]}{K_{m_1}} \tag{A1}$$

$$[ES_2] = \frac{[E][S]}{(k_5 + k_6)/k_4} = \frac{[E][S]}{K_{m_2}} \tag{A2}$$

where $[E]$ and $[S]$ are the enzyme and substrate concentrations, respectively. The rate constants, k_1, k_2, k_3, k_4, k_5, and k_6 are defined as in Fig. 3. The total concentration of enzyme, $[E_0]$, equals the sum of all the species

$$\begin{aligned}[E_0] &= [ES_1] + [ES_2] + [E] \\ &= [E]\left\{1 + \frac{[S]}{K_{m_1}} + \frac{[S]}{K_{m_2}}\right\}\end{aligned} \tag{A3}$$

Since the rates of reaction (v_1 and v_2) and the maximum velocities (V_{max_1} and V_{max_2}) are expressed as

$$v_1 = k_3[ES_1]; \qquad v_2 = k_6[ES_2] \tag{A4}$$

$$V_{max_1} = k_3[E_0]; \qquad V_{max_2} = k_6[E_0] \tag{A5}$$

then

$$\frac{v_1}{[E_0]} = \frac{k_3[ES_1]}{[E]\left\{1 + \frac{[S]}{K_{m_1}} + \frac{[S]}{K_{m_2}}\right\}} = \frac{k_3[E][S]/K_{m_1}}{[E]\left\{1 + \frac{[S]}{K_{m_1}} + \frac{[S]}{K_{m_2}}\right\}} \tag{A6}$$

Upon rearrangement of Eq. (A6), we obtain

$$v_1 = \frac{\frac{\{V_{max_1}/K_{m_1}\}}{[1/K_{m_1} + 1/K_{m_2}]}[S]}{\frac{1}{[1/K_{m_1} + 1/K_{m_2}]} + [S]} = \frac{V_{max_1}^{app}[S]}{K_{m_1}^{app} + [S]} \tag{A7}$$

where the apparent maximum velocity is

$$V_{max_1}^{app} = \frac{\{V_{max_1}/K_{m_1}\}}{[1/K_{m_1} + 1/K_{m_2}]} \tag{A8}$$

and the apparent K_m, as noted by Gillette (29), is

$$K_{m_1}^{app} = \frac{1}{[1/K_{m_1} + 1/K_{m_2}]} \tag{A9}$$

Analogously, the apparent maximum velocity and the apparent K_m for the parallel reaction are

$$V_{max_2}^{app} = \frac{\{V_{max_2}/K_{m_2}\}}{[1/K_{m_1} + 1/K_{m_2}]} \tag{A10}$$

$$K_{m_2}^{app} = \frac{1}{[1/K_{m_1} + 1/K_{m_2}]} \tag{A11}$$

The reciprocal of the apparent K_m values for formation of the two metabolites are the sum of the reciprocals of the true K_m values [Eqs. (A9) and (A11)]. When the drug is bound to blood components, as is GAM (20), the apparent K_m values equal the reciprocal of sum of the reciprocals of individual K_m values divided by the unbound fraction in blood, f_B

$$K_{m_1}^{app} = K_{m_2}^{app} = \frac{1}{\left[\frac{1}{K_{m_1}/f_B} + \frac{1}{K_{m_2}/f_B}\right]} \tag{A12}$$

The ratio of the rates of formation of metabolites arising from these two parallel pathways, v_1/v_2, becomes

$$\frac{v_1}{v_2} = \frac{V_{max_1}^{app}[S]/\{K_{m_1}^{app} + [S]\}}{V_{max_2}^{app}[S]/\{K_{m_2}^{app} + [S]\}} = \frac{V_{max_1}^{app}}{V_{max_2}^{app}} = \frac{\{V_{max_1}/K_{m_1}\}}{\{V_{max_2}/K_{m_2}\}} \tag{A13}$$

and is a quotient of the ratios of the V_{max}/K_m for the parallel pathways. A lack of concentration dependence in the ratio of metabolite formation is predicted from Eq. (A13), as noted by Gillette (29). This kind of kinetic analysis involving a single substrate, a single isozyme, and possibly a single enzymatic site and multiple products was first described by Potter *et al.* (30) for microsomal metabolism, but has not been applied to data from an intact organ. For the intact organ, the criteria for multiple product formation arising from a single isozyme are that the distributions of activities for formation of the products and the apparent K_m values must be identical [Eqs. (A9), (A11), and (A12)]. But the apparent V_{max} values for these pathways may differ [Eqs. (A8) and (A12)], resulting in ratios of products formation which are constant among all C_{In}'s and direction of flow. Because of the coupling between the same enzyme and substrate, which forms either ES_1 for ES_2 enzyme-substrate complexes (Fig. 3), this kind of parallel equilibria is distinctly different from competition reactions where two or more substrates compete for the same enzyme or enzyme site(s).

ACKNOWLEDGMENTS

We thank Dr. James R. Gillette, Laboratory of Chemical Pharmacology,

National Institutes of Health, for his invaluable suggestions on the treatment of data.

REFERENCES

1. A. M. Rappaport. The structural and functional unit in the human liver (liver acinus). *Anat. Rec.* **130:** 673-686 (1958).
2. A. M. Rappaport, Z. J. Borowy, W. M. Lougheed, and W. N. Lotto. Subdivision of hexagonal liver lobules into a structural and functional unit: Role in hepatic physiology and pathology. *Anat. Rec.* **119:** 11-34 (1954).
3. J. J. Gumucio and D. L. Miller. Functional implications of liver cell heterogeneity. *Gastroenterology* **80:** 393-403 (1981).
4. K. Jungerman and N. Katz. Functional hepatocellular heterogeneity. *Hepatology* **2:** 385-395 (1982).
5. J. L. Boyer, E. Elias, and T. J. Layden. The paracellular pathway and bile formation. *Yale J. Biol. Med.* **52:** 61-67 (1979).
6. T. Matsumara, T. Kashiwaga, H. Meren, and R. G. Thurman. Gluconeogenesis predominates in the periportal regions of the liver lobule. *Eur. J. Biochem.* **144:** 409-414 (1982).
7. T. Matsumara and R. G. Thurman. Predominance of glycolysis in pericentral regions of the liver lobule. *Eur. J. Biochem.* **140:** 229-234 (1982).
8. N. Katz. Metabolism of lipids. In R. G. Thurman, F. C. Kauffmann, and K. Jungerman (eds.), *Regulation of Hepatic Metabolism. Intra- and Intercellular Compartmentation*, Plenum Press, New York, 1986, pp. 237-252.
9. J. Baron, R. A. Redick, and F. P. Guengerich. An immunohistochemical study on the localizations and distributions of phenobarbital- and 3-methylcholanthrene-inducible cytochrome P-450 within the livers of untreated rats. *J. Biol. Chem.* **256:**5931-5937 (1981).
10. P. E. Gooding, J. Chayen, B. Sawyer, and T. F. Slater. Cytochrome P-450 distribution in rat liver and the effect of sodium phenobarbitone administration. *Chem. Biol. Interact.* **20:**299-310 (1978).
11. J. Baron, R. A. Redick, F. P. Guengerich. Immunohistochemical localization of cytochromes P-450 in rat liver. *Life Sci.* **23:**2627-2632 (1978).
12. J. A. Redick, J. Baron and F. P. Guengerich. Immunohistochical localization of glutathione-S transferases in livers of untreated rats. *J. Biol. Chem.* **257:**15200-15203 (1982).
13. K. S. Pang and J. A. Terrell. Retrograde perfusion to probe the heterogeneous distribution of hepatic drug metabolizing enzymes in rats. *J. Pharmacol. Exp. Ther.* **216:**339-346 (1981).
14. D. Ullrich, G. Fisher, N. Katz, and K. W. Bock. Intralobular distribution of UDP-glucuronosyltransferase in livers from untreated, 3-methylcholanthrene and phenobarbital-treated rats. *Chem. Biol. Interact.* **48:**181-190 (1984).
15. J. G. Conway, F. C. Kauffman, S. Ji, and R. G. Thurman. Rates of sulfation and glucuronidation of 7-hydroxycoumarin in periportal and pericentral regions of the liver lobule. *Mol. Pharmacol.* **22:**509-516 (1982).
16. J. R. deBaun, J. Y. R. Smith, E. C. Miller, and J. A. Miller. Reactivity *in vivo* of the carcinogen *N*-hydroxy-2-acetylaminoflourene: Increase by sulfate ion. *Science* **167:**184-186 (1971).
17. J. H. N. Meerman and G. J. Mulder. Prevention of the hepatotoxic action of *N*-hydroxy-2-acetylaminofluorene in the rat by inhibition of *N-O*-sulfation by pentachlorophenol. *Life Sci.* **28:**2361-2365 (1981).
18. K. S. Pang and R. N. Stillwell. An understanding of the role of enzyme localization of the liver on metabolite kinetics: A computer simulation. *J. Pharmacokin. Biopharm.* **11:**451-468 (1983).
19. K. S. Pang, H. Koster, I. C. M. Halsema, E. Scholtens, and G. J. Mulder. Aberrant pharmacokinetics of harmol in the perfused rat liver preparation: Sulfate and glucuronide conjugations. *J. Pharmacol. Exp. Ther.* **219:**134-140 (1981).

20. M. E. Morris, V. Yuen, B. K. Tang, and K. S. Pang. Competing pathways in drug metabolism. I. Effect of input concentration on the conjugation of gentisamide in the once-through *in situ* perfused rat liver preparation. *J. Pharmacol. Exp. Ther.* **245:**614–652 (1988).
21. X. Xu, B. K. Tang, and K. S. Pang. Metabolism of salicylamide in the once-through perfused rat liver preparation: Compensation by glucuronidation and hydroxylation for sulfation. *Fed. Proc.* **44:** Abs. No. 4945 (1985).
22. K. S. Pang, X. Xu, M. E. Morris and V. Yuen. Kinetic modeling of conjugations in liver. *Fed. Proc.* **46:** 2439–2441 (1987).
23. M. E. Morris and K. S. Pang. The competition between two enzymes for substrate removal in liver: Modulating effects due to substrate recruitment of hepatocyte activity. *J. Pharmacokin. Biopharm.* **15:**473–496 (1987).
24. J. G. Conway, F. C. Kauffman, T. Tsukuda, and R. G. Thurman. Glucuronidation of 7-hydroxycoumarin in periportal and pericentral regions of the liver lobule. *Mol. Pharmacol.* **25:**487–493 (1984).
25. K. S. Pang, H. Koster, I. C. M. Halsema, E. Scholtens, G. J. Mulder, and R. N. Stillwell. Normal and retrograde perfusion to probe the zonal distribution of sulfation and glucuronidation activities of harmol in the perfused rat liver preparation. *J. Pharmacol. Exp. Ther.* **224:**647–653 (1983).
26. M. E. Morris and G. Levy. Determination of salicylamide and five metabolites in biologic fluids by high performance liquid chromatography. *J. Pharm. Sci.* **72:**612–617 (1983).
27. J. A. Faust, L. J. Jules, and M. Sahyun. Derivatives of salicylamide. *J. Am. Pharm. Assoc.* (Sci. Ed.) **45:**514–517 (1956).
28. C. A. Goresky, G. G. Bach, and B. E. Nadeau. On the uptake of materials by the intact liver: the transport and net removal of galactose. *J. Clin. Invest.* **52:**991–1009 (1973).
29. J. R. Gillette. Problems in correlating *in vitro* and *in vivo* studies of drug metabolism. In L. Z. Benet, G. Levy, and B. L. Ferraiolo (eds.), *Pharmacokinetics. A Modern View*, Plenum Press, New York, 1982, pp. 235–252.
30. W. R. Potter, R. V. Branchflower and W. F. Trager. A kinetic method for the determination of multiple forms of microsomal cytochrome P-450. *Biochem. Pharmacol.* **26:**549–550 (1977).
31. J. Scholermich, S. Kitamura, and K. Miyai. Structural and functional integrity of rat liver perfused in backward and forward direction. *Res. Exp. Med.* **186:**397–405 (1986).
32. M. V. St-Pierre, W. F. Lee, W. F. Cherry, and K. S. Pang, The multiple indicator dilution technique for characterization of normal and retrograde flow in once-through rat liver perfusions. *Hepatology* (in press).
33. R. Hems, B. D. Ross, M. N. Berry, and H. A. Krebs. Gluconeogenesis in the perfused rat liver. *Biochem. J.* **101:**284–292 (1966).
34. G. M. M. Groothuis, K. P. T. Keulemans, M. J. Hardonk, and D. K. Meijer. Acinar heterogeneity in hepatic transport of dibromosulfophthalein and ouabain studied by autoradiography, normal and retrograde perfusions and computer simulations. *Biochem. Pharmacol.* **32:**3069–3078 (1983).
35. J. R. Dawson, J. G. Weitering, G. J. Mulder, R. N. Stillwell, and K. S. Pang. Alteration of transit time and direction of flow to probe the heterogeneous distribution of conjugating activities for harmol in the perfused rat liver preparation. *J. Pharmacol. Exp. Ther.* **234:**691–697 (1985).
36. E. H. Chen, J. J. Gumucio, N. H. Ho, and D. L. Gumucio. Hepatocytes of zones 1 and 3 conjugate sulfobromophthalein with glutathione. *Hepatology* **4:**467–476 (1984).
37. K. S. Pang, J. A. Terrell, S. D. Nelson, K. F. Feuer, M. J. Clements, and L. Endrenyi. An enzyme-distributed system for lidocaine metabolism in the perfused rat liver preparation. *J. Pharmacokin. Biopharm.* **14:**107–130 (1986).
38. G. M. M. Groothuis, M. J. Hardonk, K. P. T. Keulemans, P. Nieuwenhuis and D. K. F. Meijer. Autoradiographic and kinetic demonstration of acinar heterogeneity for taurocholate transport. *Am. J. Physiol.* **243:**G455–G462 (1982).
39. D. Häussinger and W. Gerok. Functional hepatocyte heterogeneity: The intracellular glutamate cycle, its regulation and physiologic significance. *J. Hepatol.* **1:**1–12 (1985).